

A multichannel model for clusters of an α and select $N = Z$ nuclei

K. Amos^{(1,4)*}, L. Canton⁽²⁾, P. R. Fraser^(1,3),
S. Karataglidis^(1,4), J. P. Svenne⁽⁵⁾, and D. van der Knijff⁽¹⁾

⁽¹⁾ *School of Physics, University of Melbourne, Victoria 3010, Australia*

⁽²⁾ *Istituto Nazionale di Fisica Nucleare,
Sezione di Padova, Padova I-35131, Italia*

⁽³⁾ *ARC Centre for Antimatter-Matter Studies,
Curtin University, GPO Box U1987,
Perth, Western Australia 6845, Australia*

⁽⁴⁾ *Department of Physics, University of Johannesburg,
P.O. Box 524 Auckland Park, 2006, South Africa and*

⁽⁵⁾ *Department of Physics and Astronomy, University of Manitoba,
and Winnipeg Institute for Theoretical Physics,
Winnipeg, Manitoba, Canada R3T 2N2*

(Dated: May 11, 2016)

Abstract

A multi-channel algebraic scattering (MCAS) method has been used to solve coupled sets of Lippmann-Schwinger equations for α +nucleus systems to find spectra of the compound systems. Low energy spectra for ^{12}C , ^{16}O , and ^{20}Ne are found with the systems considered as the coupling of an α particle with low-excitation states of the core nuclei, ^8Be , ^{12}C , and ^{16}O , respectively. Collective models have been used to define the matrices of interacting potentials. Quadrupole (and octupole when relevant) deformation is allowed and taken to second order. The calculations also require a small monopole interaction to provide an extra energy gap commensurate with an effect of strong pairing forces. The results compare reasonably well with known spectra given the simple collective model prescriptions taken for the coupled-channel interactions. Improvement of those interaction specifics in the approach will give spectra and wave functions suitable for use in analyses of cross sections for α scattering and capture by light-mass nuclei; reactions of great importance in nuclear astrophysics.

PACS numbers: 21.60Ev, 21.60Gx, 24.10Eq, 24.30Gd, 25.70Gh

*Electronic address: amos@unimelb.edu.au

I. INTRODUCTION

In light stars ($\leq 1.5 M_{\odot}$), proton-proton chain reactions lead to the formation of nuclei up to mass-8. Once the α particles generated in those reactions are present in sufficient number, the triple- α process can produce ^{12}C ; the crucial feature being the energy of the Hoyle state in ^{12}C lying just above the break-up threshold. Thereafter, α -particle captures play important roles in the catalytic C-N-O cycle of nucleogenesis. Thus the formation of light-mass nuclei by α capture at low energies, and their spectra, especially of the resonances lying above the α -breakup thresholds, are of much interest [1].

Treating nuclei as a cluster of two or more composite particles has a long history. Notably there are states of some light-mass nuclei that can be interpreted as clusters of α particles, sometimes with additional valence nucleons. The Hoyle state in ^{12}C is perhaps the most famous so treated. Clustering has been found influential particularly for states in nuclei that lie close to relevant decay thresholds [2]. Cluster model approaches also have been applied to assess the properties of the ground and sub-threshold states in nuclei; properties which often are also well described by many-nucleon models of structure. Likewise many cluster-model theories of nuclear structure and reactions have been developed with Ref. [3] being a comprehensive review. As well, there is a review [4] of the use of a complex scaling method with a cluster orbital shell model to find many-body resonances and the continua in light nuclei.

Recently, several systems of an α and an (even-even) nucleus were treated theoretically [5] with a semi-algebraic cluster model [6, 7], which accounts for Pauli-blocking of the constituent nucleons of clusters in the compound system, but only states explicitly known to be populated by these clusterisations were studied. Two of those systems, $\alpha + ^{12}\text{C}$ and $\alpha + ^{16}\text{O}$, are considered this work. Even more recently, the low-excitation, positive-parity states of ^{16}O were well described by $\alpha + ^{12}\text{C}$ clusters using the generator coordinate method with wave functions given by the antisymmetrized molecular dynamics scheme [8]. That article [8] contains an extensive set of references relating to such cluster model studies.

Herein, we consider the low-excitation spectra of ^{12}C , ^{16}O , and of ^{20}Ne by using a multi-channel algebraic scattering (MCAS) method [9] for the compound system of an α -particle interacting with low-excitation collective states of the core nuclei, ^8Be , ^{12}C , and ^{16}O , respectively. Experimental values for the states of ^8Be were taken from Ref. [10], those for ^{12}C from Ref. [11], those for ^{16}O from Ref. [12], and those for ^{20}Ne from Ref. [13]. With the current form of MCAS, descriptions of the isoscalar states in the compound systems are found. Each case in the set considered has some uniquely problematic aspects. In this, our first study of these systems using MCAS, we consider mainly the spectra of the compound nuclei. The α -emission thresholds of the three nuclei, ^{12}C , ^{16}O , and ^{20}Ne , lie between 7 and 8 MeV excitation, only a few MeV above which, the density of levels in the compound systems increases rapidly. However, MCAS is able to determine elastic scattering cross sections and we present herein also a first test estimate for an $\alpha + ^{16}\text{O}$ cross section.

We take ^8Be as the core for the cluster view of ^{12}C . The ground state of ^8Be lies just above the α -particle breakup threshold and its two lowest excited states are broad resonances. They have spin-parities 2^+ and 4^+ with energy centroids (widths) of 3.03 (1.51) MeV and of 11.35 (3.50) MeV respectively. These three resonance states of ^8Be have been considered in the coupled-channel calculation of ^{12}C taken as the $\alpha + ^8\text{Be}$ cluster. Their resonance properties are known to have an impact in cluster model evaluations of the spectra of the compound nuclei [14, 15].

Four low-lying states in ^{12}C , the ground (0^+), the 2_1^+ (4.44 MeV), the 0_2^+ (7.65 MeV), and the 3^- (9.64 MeV) have been used in our MCAS evaluations of the spectrum of the compound ^{16}O . The ground and 2_1^+ states are stable against particle emission and the two higher lying ones can decay by α emission but their widths are sufficiently small that there is only minor effects due to those aspects.

In the two evaluations mentioned above, the interaction potentials have been formed assuming a collective rotational model having isoscalar quadrupole and, with negative-parity target states, octupole deformation. An intriguing question is to find how that can lead to a low-excitation spectrum (for ^{16}O) that is usually considered as a set of vibrations upon a closed-core ground state.

Finally in treating ^{20}Ne as an $\alpha + ^{16}\text{O}$ system, besides the ground state, we have used the 0_2^+ (6.05 MeV), the 3^- (6.13 MeV), and the 2^+ (6.92 MeV) states in ^{16}O in forming the coupled-channel Hamiltonian. In this case, we have generated the interaction potentials by using a vibration model for the $\alpha + ^{16}\text{O}$ cluster and an intriguing question posed in this case is to find the more rotor-like low-energy spectrum of ^{20}Ne . In these pursuits, of course, we presume that all low-excitation isoscalar states in the compound systems, whatever their exact description, will have components that overlap with the cluster of an α and core nuclei. We presume also that only strongly coupled collective states in those core nuclei contribute importantly in defining the Hamiltonians.

A précis of the MCAS approach is given next. Then, in Sec. III, specifics of the matrix of potentials for an α +nucleus system are defined. As a first test of the $\alpha + A$ MCAS code, it was used to find spectra for ^7Li ($\alpha + ^3\text{H}$) and ^7Be ($\alpha + ^3\text{He}$); spectra found previously [16] but using a version of the code built for incident spin- $\frac{1}{2}$ particles. Test results are discussed in Sec. IV. In Sec. V, we show the results for the spectrum of ^{12}C considered as the $\alpha + ^8\text{Be}$ cluster. Sec. VI contains the MCAS results for the spectrum of ^{16}O treated as an $\alpha + ^{12}\text{C}$ system and the MCAS results for ^{20}Ne (as $\alpha + ^{16}\text{O}$) are given in Sec. VII. Finally, in Sec. VIII, MCAS results for an elastic scattering cross section of α particles from ^{16}O are shown to illustrate the utility that the approach may have in scattering data analysis. Conclusions are made in Sec. IX.

II. A PRÉCIS OF MCAS

The MCAS approach is a method to solve coupled Lippmann-Schwinger (LS) equations for a chosen two-cluster interaction matrix of potentials. The method uses separable expansions of those matrices of potentials, where a crucial choice is that of the expansion basis. The optimal choices of the form factors of those separable expansions are those derived from sturmian functions determined from the specifically-chosen two-cluster interaction matrix of potentials.

Consider a system of Γ channels for each allowed scattering spin-parity, J^π , with the index c ($= 1, \Gamma$) denoting the set of quantum numbers that identify each channel uniquely. The integral equation approach in momentum space for potential matrices, $V_{cc'}^{J^\pi}(p, q)$, requires

solution of coupled LS equations giving a multichannel T matrix of the form

$$T_{cc'}^{J^\pi}(p, q; E) = V_{cc'}^{J^\pi}(p, q) + \mu \left[\sum_{c''=1}^{\text{open}} \int_0^\infty V_{cc''}^{J^\pi}(p, x) \frac{x^2}{k_{c''}^2 - x^2 + i\epsilon} T_{c''c'}^{J^\pi}(x, q; E) dx \right. \\ \left. - \sum_{c''=1}^{\text{closed}} \int_0^\infty V_{cc''}^{J^\pi}(p, x) \frac{x^2}{h_{c''}^2 + x^2} T_{c''c'}^{J^\pi}(x, q; E) dx \right]. \quad (1)$$

Therein the contributions from open and closed channels have been separated with the respective channel wave numbers being

$$k_c = \sqrt{\mu(E - \epsilon_c)} \quad h_c = \sqrt{\mu(\epsilon_c - E)}, \quad (2)$$

for $E > \epsilon_c$ and $E < \epsilon_c$ respectively with ϵ_c being the threshold energy of channel c . Here μ designates $2m_{\text{red}}/\hbar^2$ with m_{red} being the reduced mass. With the J^π superscript understood from now on, solutions of Eq. (1) are sought using expansions of the potential matrix elements in (finite) sums of energy-independent separable terms,

$$V_{cc'}(p, q) \sim \sum_{n=1}^N \hat{\chi}_{cn}(p) \eta_n^{-1} \hat{\chi}_{c'n}(q). \quad (3)$$

With these expansions the multichannel S -matrix acquires, in general, a closed algebraic form. Indeed, the link between the multichannel T matrix and the scattering matrix is [17, 18]

$$S_{cc'} = \delta_{cc'} - i\pi\mu\sqrt{k_c k_{c'}} T_{cc'} \\ = \delta_{cc'} - i^{(l_{c'} - l_c + 1)} \pi\mu \sum_{n, n'=1}^N \sqrt{k_c} \hat{\chi}_{cn}(k_c) ([\boldsymbol{\eta} - \mathbf{G}_0]^{-1})_{nn'} \hat{\chi}_{c'n'}(k_{c'}) \sqrt{k_{c'}}, \quad (4)$$

where now c, c' refer to open channels only. In this representation, and in the case of discrete target states, \mathbf{G}_0 and $\boldsymbol{\eta}$ have matrix elements (for each value of J^π being understood)

$$[\mathbf{G}_0]_{nn'} = \mu \left[\sum_{c=1}^{\text{open}} \int_0^\infty \hat{\chi}_{cn}(x) \frac{x^2}{k_c^2 - x^2 + i\epsilon} \hat{\chi}_{c'n'}(x) dx - \sum_{c=1}^{\text{closed}} \int_0^\infty \hat{\chi}_{cn}(x) \frac{x^2}{h_c^2 + x^2} \hat{\chi}_{c'n'}(x) dx \right] \\ [\boldsymbol{\eta}]_{nn'} = \eta_n \delta_{nn'}. \quad (5)$$

The bound states of the compound system are defined by the zeros of the matrix determinant when the energy is $E < 0$ and so link to the zeros of $\{[\boldsymbol{\eta} - \mathbf{G}_0]\}$ when all channels in Eq. (5) are closed.

With coupling involving bound target states, the usual method of solution of the LS coupled equations uses the method of principal parts. However, when the target states inherent in the system are themselves resonances, the propagators in the LS coupled equations must be suitably modified [15] and direct evaluation of the integrals having complex kernels becomes possible.

III. THE MODEL FOR THE α +NUCLEUS MATRIX OF POTENTIALS

We find the α +nucleus matrix of potentials by using a collective model for the structures of the target nuclei. All terms, to second order in deformation, are carried given that the collectivity of the nucleus studied may be strong. Also, the potential field is allowed to have central (V_0), ℓ^2 -dependent ($V_{\ell\ell}$), target state spin-dependent (V_{II}), and orbit-nuclear spin ($V_{\ell I}$) components. An extra monopole interaction is allowed in the interaction between the α and the target in its ground (0^+) state.

Consider a basis of channel states defined by the coupling

$$|c\rangle = |\ell I J^\pi\rangle = \left[|\ell\rangle \otimes |\psi_I\rangle \right]_J^{M,\pi}, \quad (6)$$

where ℓ is the orbital angular momentum of relative motion of a spin-0 projectile on the target whose states are $|\psi_I^{(N)}\rangle$. With each J^π hereafter understood, and by disregarding deformation temporarily, the (α +nucleus) potential matrices may be written, as

$$V_{cc'}(r) = \langle \ell I | W(r) | \ell' I' \rangle = \left[V_0 \delta_{c'c} f(r) + V_{\ell\ell} f(r) [\ell \cdot \ell] + V_{II} f(r) [\mathbf{I} \cdot \mathbf{I}] + V_{\ell I} g(r) [\ell \cdot \mathbf{I}] \right]_{cc'} \\ + V_{mono} \delta_{c'c} \delta_{I0^+} f(r), \quad (7)$$

in which local form factors have been assumed. Typically they are specified as Woods-Saxon functions,

$$f(r) = \left[1 + e^{\left(\frac{r-R}{a}\right)} \right]^{-1} \quad ; \quad g(r) = \frac{1}{r} \frac{df(r)}{dr}. \quad (8)$$

A monopole term is included to allow $N = Z$ even-mass systems to have states in which pairing effects lead to extra binding.

Deformation then is included with the nuclear surface defined by $R(\theta, \phi) = R_0(1 + \epsilon)$ wherein ϵ is a generic term to be specified according to whether a rotational or a vibrational collective model for nuclei is used. Details are given in the appendices. Treating $R(\theta, \phi)$ as the variable in $f(r) = f(r - R(\theta, \phi))$, the function, $f(r)$, on expanding in the deformation to order ϵ^2 , becomes

$$f(r) = f_0(r) + \epsilon \left[\frac{df(r)}{d\epsilon} \right]_0 + \frac{1}{2} \epsilon^2 \left[\frac{d^2 f(r)}{d\epsilon^2} \right]_0 = f_0(r) - R_0 \frac{df_0(r)}{dr} \epsilon + \frac{1}{2} R_0^2 \frac{d^2 f_0(r)}{dr^2} \epsilon^2. \quad (9)$$

The subscript ‘0’ indicates the spherical Woods-Saxon form with $R = R_0$. There is a similar equation for $g(r)$.

More details of the expansion of these matrix elements for an α +nucleus cluster are given in Appendix A. Specifics of these potential elements when a rotation model of collectivity is used are given in Appendix B while the details relevant to use of a vibration model are given in Appendix C.

When collective models are used to specify the matrix of interaction potentials acting between a nuclear projectile and the target nucleus in which a set of states are active, there are problems in satisfying the Pauli principle [19]. In the MCAS method the effects of the Pauli principle are met by inclusion of a set of orthogonalizing pseudo-potentials (OPP) [9]; a technique that was developed in studies of cluster physics [20, 21] as a variant of the Orthogonality Condition Model (OCM) of Saito [22] and, more recently, in a study [23]

using few-body models to specify cluster structure in light nuclei. In this way, the effects of Pauli blocking in the relative motion of two clusters comprised of fermion constituents could be taken into account. The OPP can also be used for the situation with partially occupied levels being Pauli hindered. Schmid [24] notes that states can be Pauli-forbidden, Pauli-allowed, or Pauli-suppressed; the last being what we have called Pauli hindrance in MCAS theory [25–27].

To orthogonalize states describing intra-cluster motion with respect to the deeply-bound Pauli forbidden states, MCAS uses highly nonlocal OPP terms embedded in a coupled-channel context. The matrix of interaction potentials (in coordinate space) to be used has the form

$$\mathcal{V}_{cc'} = V_{cc'}(r)\delta(r - r') + \lambda_c A_c(r)A_{c'}(r')\delta_{cc'}. \quad (10)$$

$V_{cc'}(r)$ is the nuclear interaction potential and λ_c is the scale we use to give Pauli blocking. The $A_c(r)$ are bound-state wave functions of the α in the diagonal potentials, $V_{cc}(r)$, for each target state in channel c . Pauli blocking of the specific orbit in a particular channel, c , is achieved by using a very large value for λ_c . That value should be infinite but for all practical purposes 10^6 MeV suffices. Pauli allowed states have $\lambda_c = 0$ while Pauli hindrance is achieved by using intermediate values for λ_c .

IV. TEST CASES: MCAS AND $\alpha + {}^3\text{H}$, $\alpha + {}^3\text{He}$, AND $\alpha + \alpha$

These test cases are taken to be single channel problems given that the components are quite strongly bound and have no excited states below nucleon emission thresholds. But the compound systems do have well established spectra and, for the $\alpha + {}^3\text{H}$ and $\alpha + {}^3\text{He}$ systems, the states that we might expect to obtain are those indicated in Table I. The reactions involving an α that lead to them, or have the mass-7 states as a compound system, are indicated by the check marks.

TABLE I: States in ${}^7\text{Li}$ and of ${}^7\text{Be}$ relevant to this investigation and known reactions [28] involving an α that populate them.

J^π	${}^7\text{Li}$			${}^7\text{Be}$		
J^π	${}^3\text{H}(\alpha, n)$	${}^4\text{He}({}^3\text{He}, \pi^+)$	${}^4\text{He}(\alpha, p)$	${}^4\text{He}({}^3\text{He}, \gamma)$	${}^4\text{He}({}^3\text{He}, {}^3\text{He}), ({}^3\text{He}, p)$	${}^4\text{He}(\alpha, n)$
$\frac{3}{2}^-$	✓	✓	✓	✓		✓
$\frac{1}{2}^-$		✓	✓	✓		✓
$\frac{7}{2}^-$			✓		✓	
$\frac{5}{2}^-$		✓			✓	

A. The $\alpha + {}^3\text{H}$ and $\alpha + {}^3\text{He}$ systems

Spectra of ${}^7\text{Li}$ and ${}^7\text{Be}$ have been found previously [16] using the MCAS program written for spin- $\frac{1}{2}$ particles coupling to a nucleus, i.e. as ${}^3\text{H} + \alpha$ and ${}^3\text{He} + \alpha$ systems respectively. The results agreed well with known states in those spectra. Thus the first study made with the MCAS program written for α (spin-0) particles coupling to a nucleus has been of these systems but taken as an α -particle coupling to the two mass-3 systems as the core nuclei.

The interaction form specified in Eq. (7) was used with strength parameter values (in MeV),

TABLE II: Spectra of ${}^7\text{Li}$ and ${}^7\text{Be}$ from α coupled to ${}^3\text{H}$ and ${}^3\text{He}$ respectively. The energies are in MeV while the widths are in keV. The experimental values are those listed in [29]. The results labelled ‘previous’ are from [16]

J^π	${}^7\text{Li}$			${}^7\text{Be}$		
	Exp.	present	previous	Exp.	present	previous
$\frac{3}{2}^-$	spurious	-29.6	-29.4	spurious	-27.8	-28.0
$\frac{1}{2}^-$	spurious	-28.0	-27.8	spurious	-26.3	-26.4
$\frac{3}{2}^-$	-2.47	-2.59	-2.47	-1.59	-1.53	-1.53
$\frac{1}{2}^-$	-1.99	-1.87	-1.75	-1.16	-0.85	-0.84
$\frac{7}{2}^-$	2.18 (69)	2.09 (80)	2.12 (83)	2.98 (175 ± 7)	3.14 (204)	3.07 (180)
$\frac{5}{2}^-$	4.13 (918)	4.05 (800)	4.12 (834)	5.14 (1200)	5.13 (1250)	5.09 (1194)

$V_0 = -76.8$, $V_u = 1.15$, and $V_{II} = 2.34$. The geometry of the Woods-Saxon form was set with $R_0 = 2.39$ and $a = 0.68$ fm. The Coulomb potential was that from a uniformly charged sphere of radius $R_c = 2.34$ fm. A slightly larger charge radius (2.39) was used for $\alpha + {}^3\text{He}$. Using this interaction in MCAS, we obtained the results listed in Table II.

The parameter values differ (slightly) from those used previously [16] in a study of the same compound systems but taken as ${}^3\text{H}$ and ${}^3\text{He}$ coupling to an α -particle target. The differences are due primarily to use of the nuclear masses listed in [30] rather than the nucleon mass numbers. The comparison of previous with current results is sufficiently good to encourage use of the α +nucleus program for other systems.

B. The $\alpha + \alpha$ system

We have also evaluated the spectrum resulting with MCAS for the cluster, $\alpha + \alpha$; as another single-channel problem since the α particles are strongly bound and have no other bound state in the spectrum. From [28], we note that the 0_1^+ and 2_1^+ states of ${}^8\text{Be}$ have been found with the ${}^4\text{He}(\alpha, \gamma)$ and ${}^4\text{He}(\alpha, \alpha)$ reactions. With a (positive-parity) interaction [$V_0 = -46.3$ MeV, $V_u = 0.4$ MeV, $R_0 = R_c = 2.1$ fm, and $a_0 = a_c = 0.6$ fm] with MCAS, two low-excitation resonance states for ${}^8\text{Be}$ were obtained. Relative to the cluster threshold, they are the ground state (0^+) resonance having centroid and width energies of 0.095 MeV and 6 eV [c/f experimental values[29] 0.092 MeV and 5.96 eV] and a first excited (2^+) resonance state with centroid and width energies of 3.13 MeV and 1.06 MeV compared with experimental values of 3.03 MeV and 1.51 MeV respectively. With this simple (local Woods-Saxon) single channel interaction, no 4^+ resonance state is found; at least below 20 MeV excitation.

No OPP has been used in treating the $\alpha + \alpha$ cluster as a single-channel problem since all states found thereby are orthogonal. Thus any state that should be blocked because it requires the 8 nucleons to lie in the $0s$ -shell simply can be ignored. Only if there is channel coupling does a problem arise in ensuring that the Pauli principle is satisfied. With channel coupling, all resultant states of the cluster are linear combinations of all states of the same spin-parity defined in the potentials for each of the target states considered. In the present

case, the interaction has a $0s$ state bound by 21 MeV, which, due to Pauli blocking, is deemed to be spurious.

V. ^{12}C AS A COUPLED $\alpha + {}^8\text{Be}$ SYSTEM

${}^8\text{Be}$ is a particle unstable system. The ground and first two excited states are α -emissive resonances with spin-parities and centroid energies of 0^+ (ground), 2^+ at 3.03 MeV, and 4^+ at 11.35 MeV. The ground state lies only 0.092 MeV above the break-up threshold but is a long-enough lived resonance that in a stellar environment allows capture of a third α particle populating the Hoyle state in ^{12}C (0_2^+ state at 7.65 MeV). That state then γ decays to the subthreshold states and, concomitantly, is significantly responsible for the known abundance of ^{12}C . Thus any acceptable cluster model of $\alpha + {}^8\text{Be} \rightarrow {}^{12}\text{C}$ must find the Hoyle state correctly located in the spectrum.

In using MCAS to deduce the low-excitation spectrum of ^{12}C from an $\alpha + {}^8\text{Be}$ cluster, we assume that a collective rotation model prescribes the interactions of an α -particle with each state (of ${}^8\text{Be}$) considered, and forms the coupling between each of those states. The

TABLE III: The potential parameters used for the interactions in $\alpha + {}^8\text{Be}$ system. The strengths are in MeV and lengths are in fermi.

Potential		Geometry/OPP	
V_0	-39.5	$R_0 = R_c$	2.8
V_{ll}	1.5	$a_0 = a_c$	0.65
V_{II}	-1.8	β_2	-0.7
V_{III}	2.0	β_4	0.2
V_{mono}	-2.7	$\lambda_s = \lambda_p$	10^6

potential parameters for the collective model Hamiltonian for the $\alpha + {}^8\text{Be}$ cluster are listed in Table III. Values used for OPP blocking of the $\alpha + {}^8\text{Be}$ s - and p -orbits are listed as well, with the latter only of import in finding the negative-parity states of the compound. The spectrum of positive-parity states in ^{12}C that results is shown in Fig. 1. Energies shown are relative to the $\alpha + {}^8\text{Be}$ threshold. Clearly there are more evaluated states than in the observed spectrum though all those known have calculated equivalents in the vicinity of their excitation values.

With regard to these positive-parity states, the objective with the simple form for the Hamiltonian was to find the ground, 2_1^+ , and the Hoyle 0_2^+ states close to their appropriate energies relative to the $\alpha + {}^8\text{Be}$ threshold. The energies of the 2_1^+ and of the 0_2^+ states set the nuclear interaction whose parameters are listed in Table III. With that interaction the ground state was predicted to lie 5.92 MeV below threshold and to correct that to be 7.37 MeV required addition of a monopole term in the potential. Using exactly the same nuclear interaction determined to match the three low-lying positive-parity states of ^{12}C , and with full p -orbit blocking, four negative-parity states were found. Those spin-parities were 1^- , 2^- , and 3^- , as there are in the known spectrum, but the order, in particular, is not correct. By reducing the OPP strengths to have p -orbit hindrance rather than full blocking, the fully blocked results persist as long as that strength is greater than ~ 20 MeV for each target state.

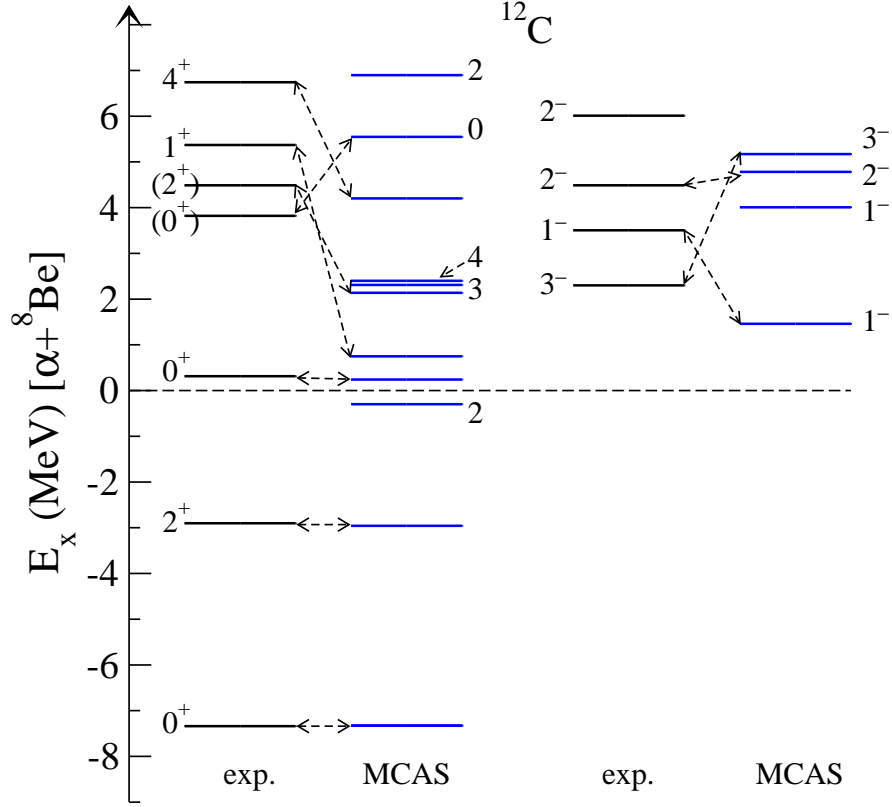


FIG. 1: (Color online) The spectrum of low-excitation states in ^{12}C . The positive-parity results are on the left while the negative-parity states are shown on the right in this figure. The MCAS results, found using the interaction Hamiltonian listed, is compared to the known set of energies (exp.).

In Fig. 2, the role of the p -orbit OPP in MCAS results for the low-excitation, isoscalar, negative-parity states in ^{12}C is displayed. The energy scale again is taken against the $\alpha + {}^8\text{Be}$ threshold. The known values are shown in the column labelled ‘exp’. These first MCAS results were found using exactly the same nuclear interaction determined to match the three low-lying positive-parity states of ^{12}C . The various MCAS results, labelled ‘(a)’ through ‘(e)’ were found by using diverse OPP blocking of the p -orbit in each of the three target states (of ${}^8\text{Be}$) chosen in the calculations. Full p -orbit blocking in all three states gave the results shown in column (a). The MCAS spectrum found when no blocking of the p -orbit is made is shown in column (b), in which there are numerous sub-threshold negative-parity states. The same four resonance states are there though, as they are in each of the other calculated spectra in this figure. The results shown in columns (c), (d), and (e) respectively were obtained by making the p -orbit unblocked for the incident α in the ground, the 2^+ state, and the 4^+ states of the target (${}^8\text{Be}$) respectively. Without the ground state OPP a deep lying 1^- bound state ensues. Without the p -orbit blocking in the 2^+ state interactions, a triplet of bound states of spin-parities 1^- , 2^- and 3^- is found. While without any such blocking with the target 4^+ state, extra 3^- and 4^- bound states appear.

Small variations of the non-central interaction strengths did not improve the results. In fact, to get the correct order for the isoscalar, negative-parity resonances in ^{12}C , the negative-parity interaction had to be varied markedly from that used to get the positive-parity states.

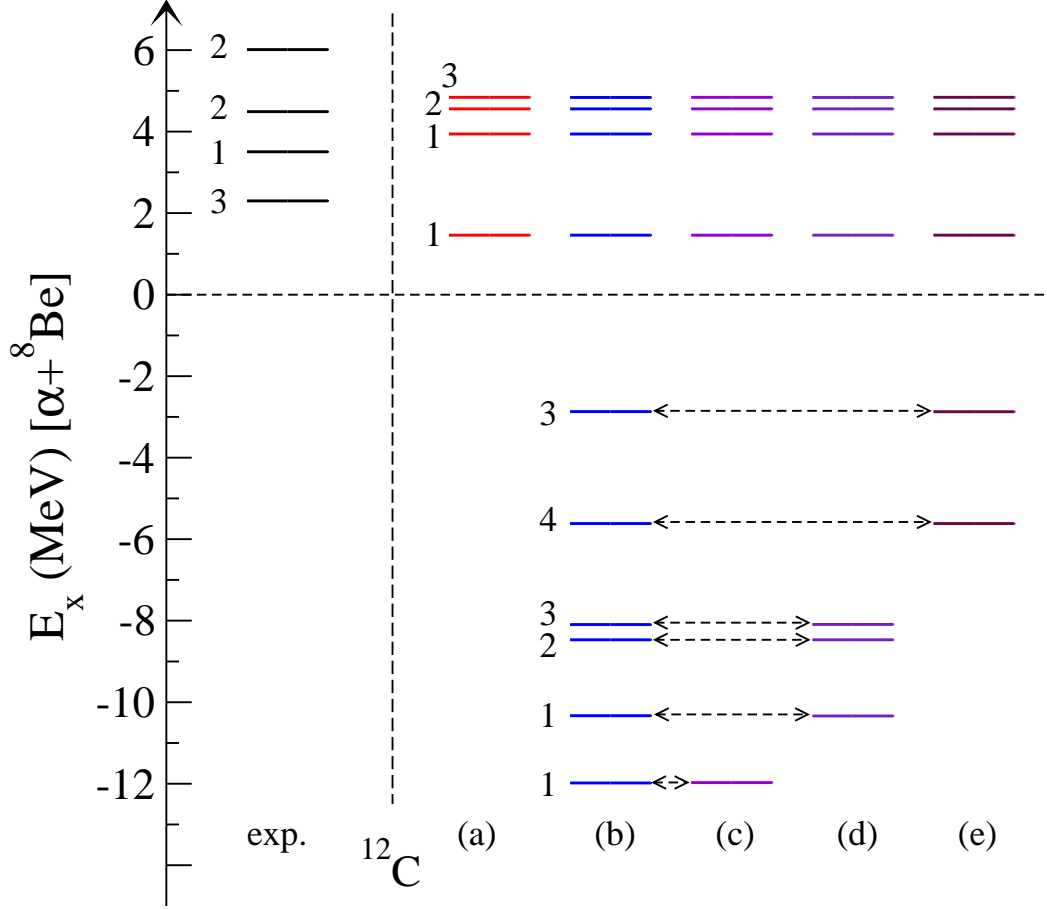


FIG. 2: (Color online) The negative-parity spectrum of ^{12}C in relation to the $\alpha + {}^8\text{Be}$ threshold. The MCAS result found using the interaction Hamiltonian listed compared to the known set of state energies (exp.). Details are given in the text.

Even then the known energy gaps were not well reproduced and extra (not observed) states were found in the low-excitation region considered.

The full set of results are presented in Table IV with the widths of resonances (in keV) listed along with their energy centroids (in MeV). The states are listed in the order in which they were found from the MCAS evaluations and compared with experimental values. The widths of the evaluated resonance states are strongly affected by the widths of the 2^+ and 4^+ states in ${}^8\text{Be}$ (the experimental values were used in the calculations). If one were to treat those as sharp (zero width) then the resultant resonance widths are many orders of magnitude smaller; some even reflecting bound states in the continuum. Strong influence on resonance widths of a compound nucleus, ${}^9\text{Be}$ (as $n + {}^8\text{Be}$), due to the target states themselves being resonances was observed using MCAS [15].

However, these results from this $\alpha + {}^8\text{Be}$ study leave much to be desired and that reflects the difficulty of the model prescription in which the α coupled to states of the notably deformed and unstable target attempting to replicate states of the particularly stable compound system, ^{12}C .

TABLE IV: Known and MCAS spectral properties of low-excitation states in ^{12}C . Widths are in keV, centroids in MeV.

J^π	E_{exp}	Γ_{exp}	E_{MCAS}	Γ_{MCAS}
0^+	-7.37	—	-7.37	—
2^+	-2.93	—	-2.95	—
2^+			-0.30	—
0^+	0.28	~ 0.008	0.24	750
3^+			2.29	760
4^+			2.43	1800
2^+	3.79	430 ± 80	2.15	762
1^+	5.34	0.02	0.75	750
4^+	6.71	258 ± 15	4.23	770
3^-	2.30	35 ± 5	1.81	9.2
1^-	3.50	315 ± 25	2.04	1085
2^-	4.49	260 ± 25		
2^-	5.98	375 ± 40	6.05	2800

VI. ^{16}O AS A COUPLED $\alpha + ^{12}\text{C}$ SYSTEM

Over 35 years ago, semi-microscopic and microscopic $\alpha + ^{12}\text{C}$ cluster models were used, refs. [31–34] for example, to study excited states of ^{16}O . It was found that many could be described by $\alpha + ^{12}\text{C}$ cluster structures. Studies of that nature remain topical as, in a recent article [8], cluster structures for positive-parity states of ^{16}O were investigated using the generator coordinate method and an extended $\alpha + ^{12}\text{C}$ cluster model. The ground and excited states of ^{12}C were taken into account by using wave functions defined by the antisymmetrized molecular dynamics method. The 0_2^+ , 2_1^+ and 4_1^+ states of ^{16}O were described well and those cluster states were found to be dominated by the $\alpha + ^{12}\text{C}(0_1^+)$ structure.

There are five states in ^{16}O lying below the $\alpha + ^{12}\text{C}$ threshold of 7.16 MeV. All can be populated in $^{12}\text{C}(\alpha, \gamma)$ reactions [28]. Thus we anticipated that MCAS evaluations could give estimates of the low-lying excitation spectrum of ^{16}O .

Three states in ^{12}C have been used previously in defining a coupled-channel Hamiltonian for the mirror pair, ^{13}C and ^{13}Na , as nucleon+ ^{12}C systems. The spectra of those compound systems were well reproduced [9]. The three states used were the ground (0^+), the first excited (2^+) at 4.44 MeV, and the second excited (0^+) at 7.65 MeV. Low-energy cross sections and analysing powers from the scattering of nucleons from ^{12}C were also well reproduced [9].

To study the $\alpha + ^{12}\text{C}$ system, we also include the 3^- (9.64 MeV) state in ^{12}C to specify the diverse channels in the coupled-channel model used. Quadrupole and octupole deformations have been used to specify the coupling between states and the interaction strengths are listed in Table V. Further, to define a spectrum for ^{16}O from the cluster of an α and ^{12}C we need to use Pauli blocking and/or Pauli hindrance of the s and p -orbits. The values of the OPP strengths used for that are listed in Table VI.

Using the matrix of interaction potentials formed with these parameter values gives the spectrum for ^{16}O shown in Fig. 3. The sub-threshold states are in very good agreement with the known values as they were used to ‘tune’ the interaction parameters for both parities.

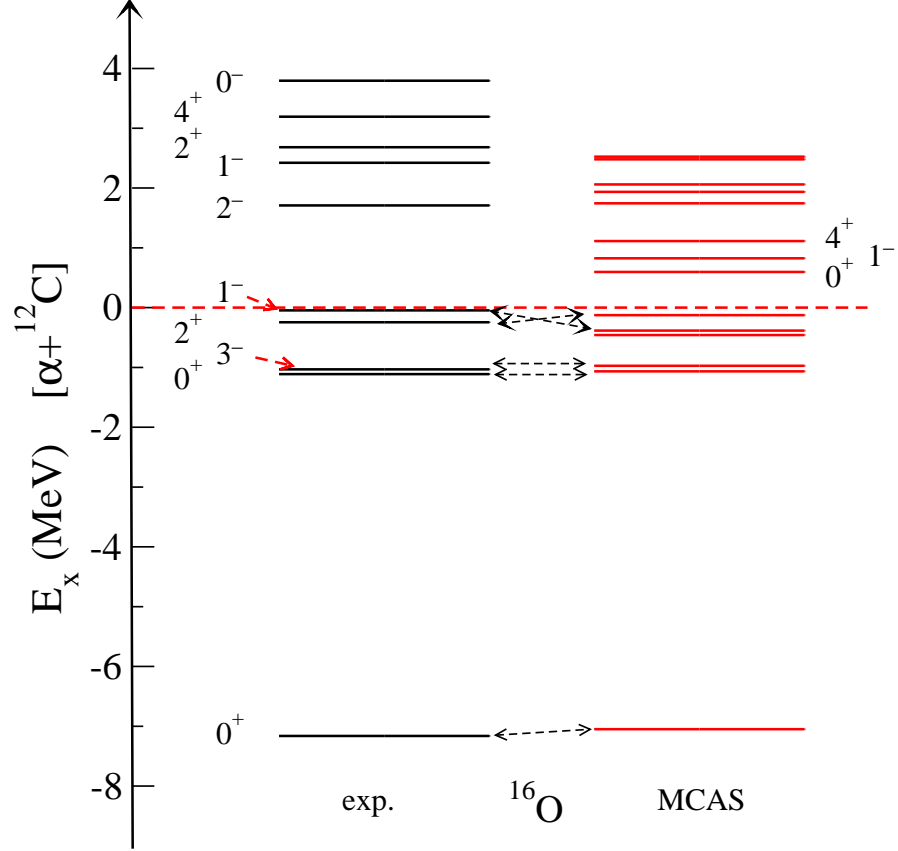


FIG. 3: (Color online) The spectrum of ^{16}O in relation to the $\alpha + ^{12}\text{C}$ threshold. The MCAS result found using the interaction Hamiltonian listed compared to the known set of state energies (Exp.).

TABLE V: The parameters defining the MCAS Hamiltonian potential for the $\alpha + ^{12}\text{C}$ system. Energies and lengths are in MeV and fermi respectively.

Type	odd parity	even parity
V_0	-27.0	-30.0
$V_{\ell\ell}$	1.2	5.0
$V_{\ell I}$	1.0	-5.0
V_{II}	0.0	0.7
V_{mono}	—	-3.5
Geometry:	$R = R_c = 3.4$	$a = a_c = 0.6$
Deformation:	$L = 2$	$\beta_n = \beta_c = -0.52$
	$L = 3$	$\beta_n = \beta_c = 0.37$

Most notable was the monopole term since only with that component could the splitting of the ground to first excited state be determined. Clearly, though, this model fails to give an adequate spread of resonance states. Nonetheless, each spin-parity state in the known spectrum (other than the particularly unique unnatural-parity 0^- state) has a matching member in the MCAS result.

TABLE VI: The orthogonalising pseudo-potential strengths in MeV.

state	0_{gs}^+	$2^+(4.4389)$	$0^+(7.654)$	$3^-(9.641)$
s -wave	10^6	10^6	11.0	11.0
p -wave	9.0	3.0	3.0	0.0

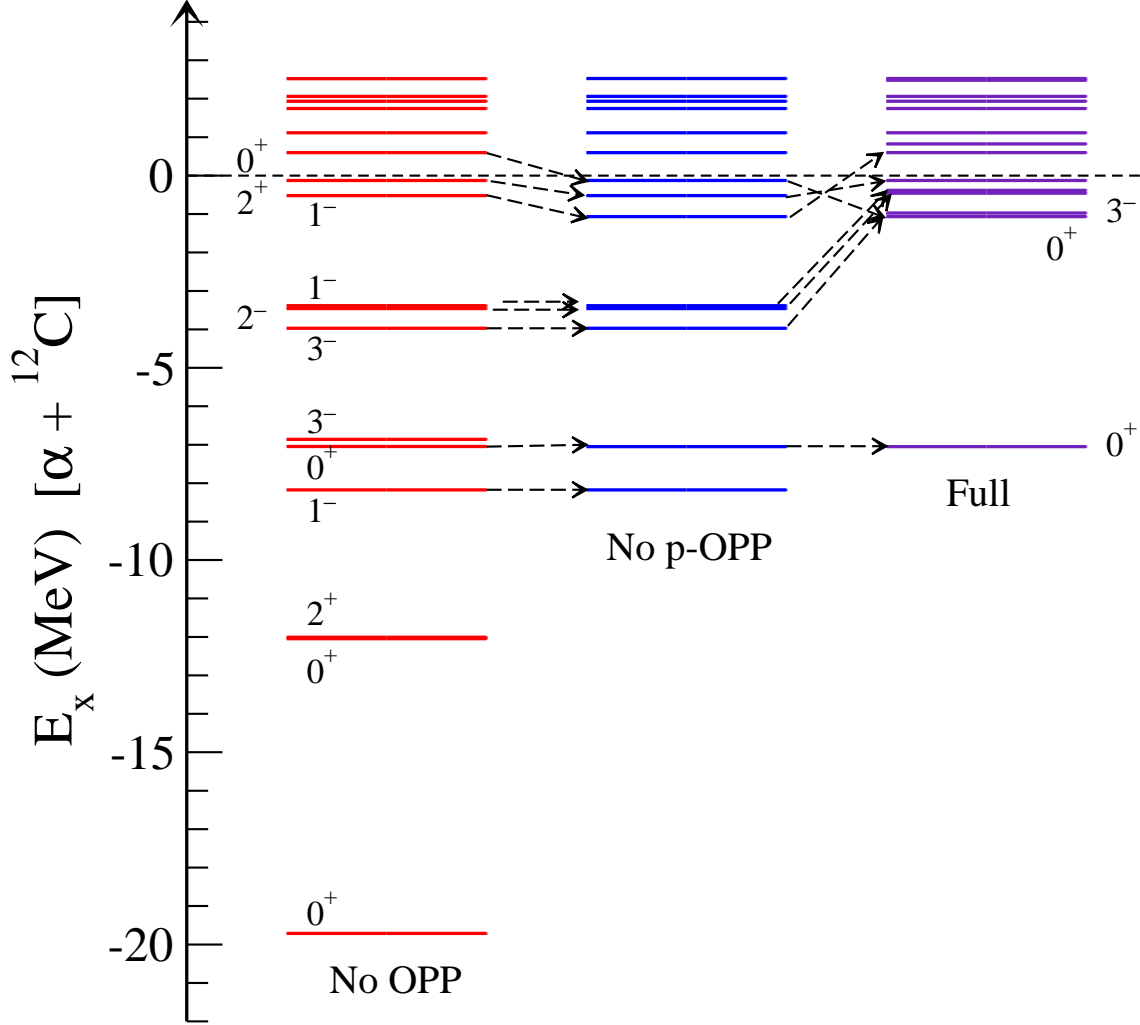


FIG. 4: (Color online) MCAS spectra found using the defined nuclear and Coulomb interactions and with no OPP included (left), with the p -OPP strengths in all four states set to zero (middle), compared with the full result (right) as given in Fig. 3.

In Fig. 4, the effects of changing the various strength values of the OPP entries in the Hamiltonian are shown. With each case, the specific set and order of the finite number of sturmians used to expand the interaction matrix of potentials, change. Concomitantly the components of the coupled-channel states displayed in the spectra will also change. Certainly the admixtures of those components in each compound state found will vary. Thus the dashed lines connecting the states in this figure should only be taken as identification of the state spin-parity in each spectrum.

VII. ^{20}Ne AS A COUPLED $\alpha + ^{16}\text{O}$ SYSTEM

The $\alpha + ^{16}\text{O}$ threshold in ^{20}Ne lies at 4.73 MeV excitation and just the ground (0^+), first excited (2^+), and second excited (4^+) states of ^{20}Ne are subthreshold. They are all populated by $^{16}\text{O}(\alpha, \gamma)$ processes. Using MCAS to study the cluster system seems straightforward but there is the question of how adding an α to a system (^{16}O) often thought to have collective attributes of vibrational model character can achieve a spectrum (of ^{20}Ne) that has collective attributes reminiscent of a rotational model.

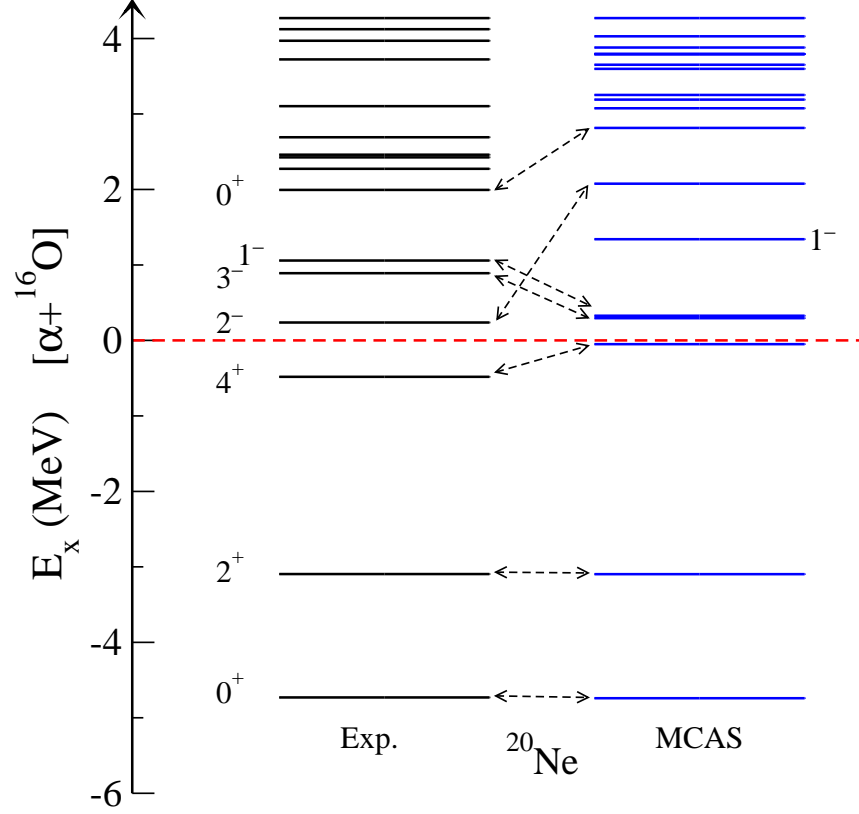


FIG. 5: (Color online) MCAS spectrum for ^{20}Ne as an $\alpha + ^{16}\text{O}$ cluster compared to the known one referenced against the $\alpha + ^{16}\text{O}$ threshold.

The coupled-channel problem has been treated with MCAS by considering the interactions with a vibration model for five low-excitation states in ^{16}O . Besides the ground (0^+) state treated as the vibration vacuum, we have included the 0_2^+ (6.05 MeV) state as a two quadrupole phonon excitation, the 3^- (6.13 MeV) state as a single octupole excitation, the 2^+ (6.92 MeV) state as a single quadrupole excitation, and the 1^- (7.12 MeV) state as a two phonon (quadrupole plus octupole) excitation. We also assumed that the bound s and p -orbits were blocked by using the OPP weights, $\lambda_s = \lambda_p = 10^6$ MeV. Then on using the parameter set listed in Table VII, the resulting spectrum is shown in Fig. 5 in comparison with the known one. In this case, no $V_{\ell I}$ component was needed to get the spectrum labelled MCAS in the figure.

The seven lowest excitation states in the known spectrum have matching entries in the MCAS result and, with the exception of the unnatural-parity 2_1^- state, they agree to better

TABLE VII: The parameters defining the MCAS Hamiltonian potential for the $\alpha + {}^{16}\text{O}$ system. Energies and lengths are in MeV and fermi respectively.

Type	Negative	Positive	Geometry
V_0	-26.0	-27.2	$R = R_c = 3.4$
$V_{\ell\ell}$	0.16	0.16	$a = a_c = 0.65$
V_{II}	-0.19	-0.19	$L = 2 ; \beta_n = \beta_c = 0.52$
V_{mono}		-0.23	$L = 3 ; \quad = 0.4$

than an MeV. The evaluated 4_1^+ state is just bound while the low-lying 3^- and 1^- resonant states are in the observed order but their centroid energies are close and smaller than is observed. Also the calculated spectrum has an additional 1^- resonance whose centroid is at 1.34 MeV. The known 1_2^- resonance centroid is at 4.12 MeV in this figure.

The full set of results are presented in Table VIII with the widths of resonances (in keV) listed along with their energy centroids (in MeV). With one exception, MCAS finds

TABLE VIII: Known and MCAS spectral properties of low-excitation states in ${}^{20}\text{Ne}$. Widths are in keV, centroids in MeV.

J^π	E_{exp}	Γ_{exp}	E_{MCAS}	Γ_{MCAS}
0_1^+	-4.73	—	-4.74	—
2_1^+	-3.09	—	-3.10	—
4_1^+	-0.48	—	-0.05	—
2_1^-	0.24	γ -decay	2.08	$< 10^{-13}$
3_1^-	0.89	\pm	0.30	3×10^{-13}
1_1^-	1.09	$(2.8 \pm 0.3) 10^{-2}$	0.33	$< 10^{-13}$
0_2^+	2.00	19 ± 0.9	2.82	230
1_2^-	3.98	19	1.34	0.32
4_1^-	2.27	γ -decay	3.88	$< 10^{-13}$
3_2^-	2.43	8.2 ± 0.3	3.19	4
0_3^+	2.46	3.4 ± 0.2	3.08	820
2_2^+	2.69	15.1 ± 0.7	3.65	228
2_3^+	3.10	2	4.03	105
5_1^-	3.72	0.013		
0_4^+	~ 4	> 800	3.25	40

all states additional to those labelled explicitly in Fig. 5 to within an MeV of the tabulated data. The exception is the 4_1^- state but as this only decays by γ emission it may not be well described as an α cluster model. The widths of the resonances are not well matched by the simple model calculation and that points to the need for a better prescription of the coupled-channel Hamiltonian.

VIII. MCAS AND ELASTIC SCATTERING OF α PARTICLES

Besides producing bound and resonant state expectations for the spectrum of the compound system studied, MCAS can determine scattering matrices for energies above the particular cluster threshold, and thus, cross sections. In the past, for the compound systems ^{13}C (treated as $n+^{12}\text{C}$) [9], and ^{15}F (treated as $p+^{14}\text{O}$) [25], scattering cross sections were obtained that were in very good agreement with measured data. Even spin-dependent measurable data were matched in the former, and resonances were predicted with the latter, some of which were subsequently discovered [35, 36].

Much data has been taken for low-energy scattering of α particles, from ^{12}C and ^{16}O in particular, and resonance features are very evident in the associated elastic scattering cross sections. That is especially the case at backward scattering angles. We show just one example herein, namely that of elastic scattering of α particles from ^{16}O taken at 165° and for energies between 2 and 6 MeV, simply to illustrate the utility of MCAS to determine scattering cross sections.

Two data sets and our MCAS result are shown in Fig. 6. Clearly the known detailed structure is not reproduced, but that was not unexpected since, as yet, the Hamiltonian does not give resonant states of the compound (^{20}Ne) sufficiently in agreement with the known spectrum. That is the case with $\alpha + ^{12}\text{C}$ scattering as well, and for the same reason. However, with the example shown, the average magnitude of the cross section and of the evaluated resonant structures in the energy range are comparable in magnitude and width with those in the data. These results serve encourage to find improved model coupled-channel interactions, to those from the quite simple collective models we have used to date, to find better evaluated spectra of the compound systems.

IX. CONCLUSIONS

The MCAS method has been used to define low-energy spectra for ^{12}C , ^{16}O , and ^{20}Ne with the systems considered as the coupling of an α particle with low-excitation states of the core nuclei, ^8Be , ^{12}C , and ^{16}O , respectively. Collective models have been used to define the matrices of interacting potentials and quadrupole (and octupole when relevant) deformation allowed and taken to second order. The program was checked by it replicating results found previously with a version built to describe spin- $\frac{1}{2}$ nuclei clustered with nuclei having ground state spin-parity 0^+ . Results of the single-channel $\alpha + \alpha$ cluster found the essential known states of ^8Be in good agreement with the known spectrum.

Treating ^{12}C as an $\alpha + ^8\text{Be}$ cluster required a monopole term (strength -2.7 MeV) to achieve a good replication of the ground, 2^+ (4.44 MeV), and the just unbound 0_2^+ (7.65 MeV) states; the extremely narrow width of that 0_2^+ was not matched however. All other known resonance states to ~ 12 MeV were found to have partners in the MCAS spectrum but without a close match. The results reflected the difficulty of using a simple model cluster prescription in seeking a spectrum of a particularly stable compound nucleus when one of the elements is a strongly deformed and unbound nucleus. Treating ^{16}O as a cluster of an α with the quite stable ^{12}C led to a good match for the sub-threshold (for α breakup) bound states of the compound. Again a monopole term (strength -3.5 MeV) was required to depress the ^{16}O ground state below the next set of its excited ones. Resonance states found with MCAS match spin-parities of the quintuplet of resonances in the known spectrum but with energy centroids 1 – 2 MeV too small.

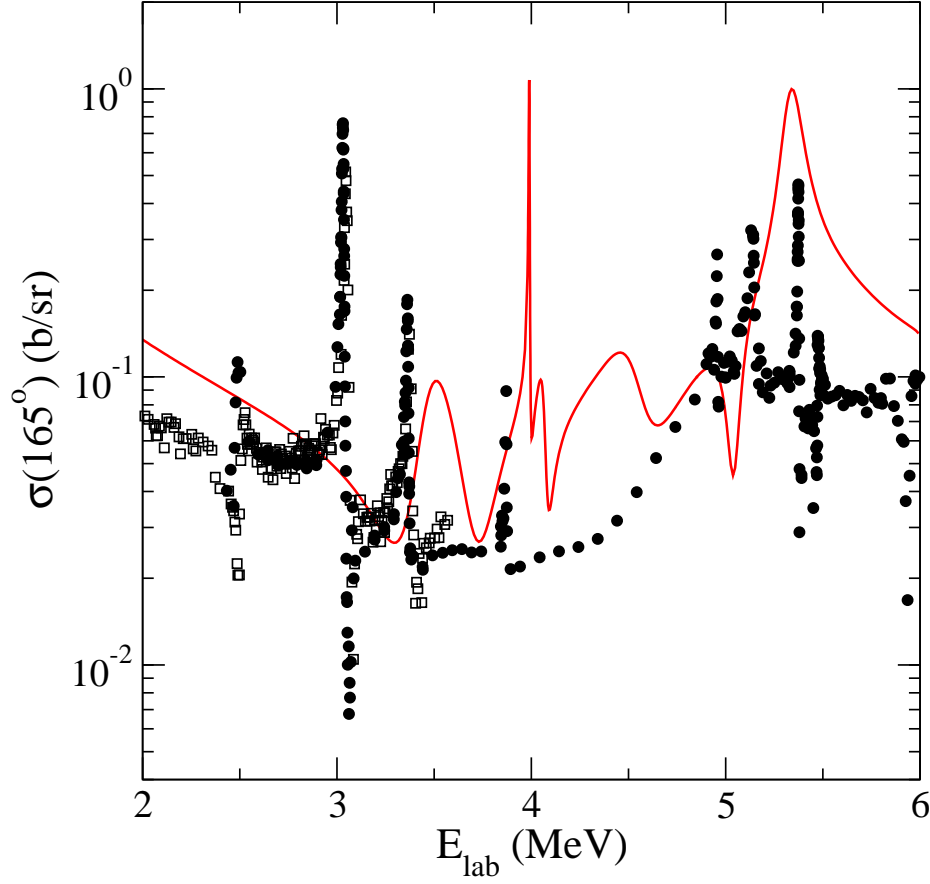


FIG. 6: (Color online) Cross sections for $\alpha + {}^{16}\text{O}$ elastic scattering at 165° for a range of incident α -particle energies. The MCAS result (solid curve) is compared with two data sets; the filled circles are the data of [37] while the open squares are those of [38].

We considered ${}^{20}\text{Ne}$ as a coupled-channel problem of an α with the low-excitation spectrum of ${}^{16}\text{O}$. The interactions in this case were specified using a pure vibration model for the core nucleus. In this study the role of Pauli blocking of some α -particle states from the coupled-channel problem was essential in finding the resultant spectrum in agreement with the known one, having three subthreshold states with energies reminiscent of a rotation model. The lowest known resonance states have partners in the MCAS result though, once more, the energy centroids are 1 – 2 MeV from matching and the widths found are not in good agreement with the tabulated ones.

Finally, as an example of the utility in using MCAS to define scattering cross sections, an MCAS result for low-energy α -particle elastic scattering from ${}^{16}\text{O}$ was compared with data taken at 165° . The same multi-channel interaction used to get the spectrum of ${}^{20}\text{Ne}$ was used and so observed resonance states were not matched. Nonetheless the average magnitude of the evaluated cross section is comparable to the measured one and resonance shapes and magnitudes obtained using MCAS are similar to the measured ones save that they are not at the observed energies. These characteristics we can expect to improve as better model interactions are used in the coupled-channel Hamiltonian.

Each of the systems studied has some aspects that concur with the known compound system low-excitation spectrum when a monopole term is included in the interaction matrix

of potentials. This extra term we believe is a reflection of strong pairing in the ground states of the $N = Z$ compound nuclei considered. Each cluster has unique problematic aspects for treatment with the simple collective model prescriptions for the interactions of an α particle with the core nuclei. ^8Be is an unbound system not only having resonance states but it is also strongly deformed. ^{12}C has a rotor like low-excitation spectrum but the compound, ^{16}O , has a low-excitation spectrum reminiscent of a vibrations on a spherical ground state. Then the $\alpha + ^{16}\text{O}$ cluster seeks to form ^{20}Ne whose low-excitation spectrum seems to have rotor like characteristics. Nonetheless, with reasonable interactions and orthogonalising pseudo-potentials accounting for credible Pauli blocking of the the relative motion of nucleons in the α +nucleus clusters, these most simple prescriptions of the coupled-channel problems give good descriptions of sub-threshold states in the compound systems, and of some resonance states. This makes further investigations with MCAS leading to assessments of low-energy α -capture processes worthwhile.

Acknowledgments

JPS acknowledges support from the Natural Sciences and Engineering Research Council of Canada. SK acknowledges support from the National Research Foundation of South Africa. PRF acknowledges funds from the Dipartimento di Fisica e Astronomia dell'Universit di Padova and the PRIN research project 2009TWL3MX, and of helpful conversations with Peter O. Hess.

Appendix A: Collective models of α +nucleus potential matrices

For an α +nucleus cluster system, the symmetrized form of the matrix of interaction potentials to be used is

$$\begin{aligned}
V_{cc'}(r) &= V_0 f_{cc'}(r) + \frac{1}{2} V_{\ell\ell} \sum_{c''} \left([\ell \cdot \ell]_{cc''} f_{c''c'}(r) + f_{cc''}(r) [\ell \cdot \ell]_{c''c'} \right) \\
&\quad + \frac{1}{2} V_{II} \sum_{c''} \left([\mathbf{I} \cdot \mathbf{I}]_{cc''} f_{c''c'}(r) + f_{cc''}(r) [\mathbf{I} \cdot \mathbf{I}]_{c''c'} \right) \\
&\quad + \frac{1}{2} V_{\ell I} \sum_{c''} \left([\ell \cdot \mathbf{I}]_{cc''} g_{c''c'}(r) + g_{cc''}(r) [\ell \cdot \mathbf{I}]_{c''c'} \right) \\
&= \left[V_0 + \frac{1}{2} V_{\ell\ell} \left(\ell'(\ell' + 1) + \ell(\ell + 1) \right) + \frac{1}{2} V_{II} \left(I'(I' + 1) + I(I + 1) \right) \right] f_{cc'}(r) \\
&\quad + \frac{1}{4} V_{\ell I} \left(2J(J + 1) - \ell'(\ell' + 1) - \ell(\ell + 1) - I'(I' + 1) - I(I + 1) \right) g_{cc'}(r),
\end{aligned}$$

since,

$$\begin{aligned}
[\ell \cdot \ell]_{cc'} &= \sum_{m_\ell m_{\ell'} N N'} \langle \ell I m_\ell N | J M \rangle \langle \ell' I' m_{\ell'} N' | J M \rangle < \ell m_\ell \left| \vec{l}^2 \right| \ell' m_{\ell'} > \delta_{I' I} \delta_{N' N} \\
&= \ell(\ell + 1) \sum_{m_\ell N} [\langle \ell I m_\ell N | J M \rangle]^2 \delta_{I' I} \delta_{N' N} \delta_{\ell' \ell} \delta_{m_\ell m_{\ell'}} = \ell(\ell + 1) \delta_{cc'}, \tag{A1}
\end{aligned}$$

and likewise $[\mathbf{I} \cdot \mathbf{I}]_{cc'} = I(I+1)\delta_{cc'}$. Similarly one finds that, for α +nucleus systems as $\ell + \mathbf{I} = \mathbf{J}$ is conserved,

$$[\ell \cdot \mathbf{I}]_{cc''} = \frac{1}{2} [J(J+1) - \ell(\ell+1) - I(I+1)] \delta_{cc''} . \quad (\text{A2})$$

Appendix B: Using a rotation model of the target

The surface of a rigid drop of matter, with permanent, but axially symmetric, deformation from the spherical, is represented by the expansion

$$R = R_0 \left[1 + \sum_L c_L P_L(\theta') \right] , \quad (\text{B1})$$

where the angles refer to a body fixed symmetry axis, ϕ' being understood. The C_L are suitable coefficients to form the chosen shape of the surface of the nucleus. This transforms to a space-fixed frame to take the form

$$R = R_0 \left[1 + \sum_L \sqrt{\frac{4\pi}{(2L+1)}} \beta_L [\mathbf{Y}_L(\Omega) \cdot \mathbf{Y}_L(\xi)] \right] , \quad (\text{B2})$$

where $\Omega(\theta\phi)$ refer to the space-fixed axis and ξ are the Euler angles of the transformation and β_L are the usual deformation parameters. Even with odd-mass nuclei for which the states will have half-integer spin, we will presuppose that collective excitation is of the underlying even-mass core.

A rotor model prescription for $f(r)$, with deformation

$$\epsilon = \sum_L \sqrt{\frac{4\pi}{(2L+1)}} \beta_L [\mathbf{Y}_L(\Omega) \cdot \mathbf{Y}_L(\xi)] \quad (\text{B3})$$

taken to second order, gives a channel-space matrix

$$\begin{aligned} f_{cc'}(r) &= \left\{ f_0(r) - R_0 \frac{df_0(r)}{d\epsilon} \sum_L \sqrt{\frac{4\pi}{(2L+1)}} \beta_L [\mathbf{Y}_L(\Omega) \cdot \mathbf{Y}_L(\xi)] \right. \\ &\quad + R_0^2 \frac{d^2 f_0(r)}{d\epsilon^2} \sum_{L_1, L_2} \frac{4\pi}{\sqrt{(2L_1+1)(2L_2+1)}} \beta_{L_1} \beta_{L_2} \\ &\quad \left. \times [\mathbf{Y}_{L_1}(\Omega) \cdot \mathbf{Y}_{L_1}(\xi)] [\mathbf{Y}_{L_2}(\Omega) \cdot \mathbf{Y}_{L_2}(\xi)] \right\}_{cc'} \\ &= [f_0(r)]_{cc'} - R_0 \frac{df_0(r)}{dr} \sum_L \sqrt{\frac{4\pi}{(2L+1)}} \beta_L [\mathbf{Y}_L(\Omega_r) \cdot \mathbf{Y}_L(\xi)]_{cc'} \\ &\quad + \frac{1}{2} R_0^2 \frac{d^2 f_0(r)}{dr^2} \left[\sum_{L_1 L_2} \sqrt{(2L_1+1)(2L_2+1)} \beta_{L_1} \beta_{L_2} \right. \\ &\quad \left. \times \sum_{\mathcal{L}} \frac{1}{(2\mathcal{L}+1)} [\langle L_1 L_2 00 | \mathcal{L} 0 \rangle]^2 [\mathbf{Y}_{\mathcal{L}}(\Omega_r) \cdot \mathbf{Y}_{\mathcal{L}}(\xi)]_{cc'} \right] , \quad (\text{B4}) \end{aligned}$$

where we have used the identity

$$\begin{aligned} & [\mathbf{Y}_{L_1}(\Omega) \cdot \mathbf{Y}_{L_1}(\xi)] [\mathbf{Y}_{L_2}(\Omega) \cdot \mathbf{Y}_{L_2}(\xi)] \\ &= \frac{1}{4\pi} (2L_1 + 1) (2L_2 + 1) \sum_{\mathcal{L}} \frac{1}{2\mathcal{L} + 1} [\langle L_1 L_2 00 | \mathcal{L} 0 \rangle]^2 [\mathbf{Y}_{\mathcal{L}}(\Omega) \cdot \mathbf{Y}_{\mathcal{L}}(\xi)]. \end{aligned} \quad (\text{B5})$$

Then the potentials are

$$\begin{aligned} V_{cc'}(r) = & \left[\left(V_0 + V_{\ell\ell} \ell(\ell + 1) + V_{II} I(I + 1) \right) f_0(r) \right. \\ & \left. + \frac{1}{2} V_{\ell I}(r) \left(J(J + 1) - \ell(\ell + 1) - I(I + 1) \right) g_0(r) \right] \delta_{cc'} \\ & - R_0 \left[\frac{df_0(r)}{dr} \left(V_0 + \frac{1}{2} V_{\ell\ell} [\ell'(\ell' + 1) + \ell(\ell + 1)] + \frac{1}{2} V_{II} [I'(I' + 1) + I(I + 1)] \right) \right. \\ & \left. + \frac{1}{4} \frac{dg_0(r)}{dr} V_{\ell I} \left(2J(J + 1) - \ell'(\ell' + 1) - \ell(\ell + 1) - I'(I' + 1) - I(I + 1) \right) \right] \\ & \times \sqrt{(2\ell' + 1)} \sum_L \beta_L (-1)^{(\ell' + I + J)} \langle \ell' L 00 | \ell 0 \rangle \left\{ \begin{matrix} I & L & I' \\ \ell' & J & \ell \end{matrix} \right\} \\ & \times < I' \| \mathbf{Y}_L \| I > \\ & + \frac{1}{2} R_0^2 \left[\frac{d^2 f_0(r)}{dr^2} \left(V_0 + \frac{1}{2} V_{\ell\ell} [\ell'(\ell' + 1) + \ell(\ell + 1)] + \frac{1}{2} V_{II} [I'(I' + 1) + I(I + 1)] \right) \right. \\ & \left. + \frac{1}{2} \frac{d^2 g_0(r)}{dr^2} V_{\ell I} \left(2J(J + 1) - \ell'(\ell' + 1) - \ell(\ell + 1) - I'(I' + 1) - I(I + 1) \right) \right] \\ & \times (-1)^{(\ell' + I + J)} \frac{1}{\sqrt{4\pi}} \sqrt{(2\ell' + 1)} \sum_{L_1 L_2} \beta_{L_1} \beta_{L_2} \sqrt{(2L_1 + 1)(2L_2 + 1)} \\ & \times \sum_{\mathcal{L}} \frac{1}{\sqrt{(2\mathcal{L} + 1)}} [\langle L_1 L_2 00 | \mathcal{L} 0 \rangle]^2 \langle \ell' \mathcal{L} 00 | \ell 0 \rangle \left\{ \begin{matrix} I & \mathcal{L} & I' \\ \ell' & J & \ell \end{matrix} \right\} \\ & \times < I \| \mathbf{Y}_{\mathcal{L}} \| I' >. \end{aligned}$$

Note we have retained all terms in the phase factor since I' may be integer or half-integer.

To find the structure factors in the above, consider the Hamiltonian for a general quantum rotor to be

$$H_{total} = H + H_{intrinsic} \quad ; \quad H = H_{rot} = \frac{\hbar^2}{2} \left[\frac{1}{\mathcal{I}_1} L_1^2 + \frac{1}{\mathcal{I}_2} L_2^2 + \frac{1}{\mathcal{I}_3} L_3^2 \right], \quad (\text{B6})$$

where the moment of inertia are about body fixed axes with 3 taken to be the equivalent to the space-fixed z -axis. An intrinsic Hamiltonian has been included though we will assume that the intrinsic state does not change with the low-excitation states to be considered.

The basic eigenvectors $|LMK\rangle$ satisfy

$$\mathbf{L}^2 |LMK\rangle = L(L + 1) |LMK\rangle, \quad L_z |LMK\rangle = M |LMK\rangle, \quad \text{and} \quad L_3 |LMK\rangle = K |LMK\rangle. \quad (\text{B7})$$

The adiabatic condition is assumed so that the intrinsic and rotational degrees of freedom decouple. Then, for a rotor in general having no axis of symmetry, its eigenstates will have the form

$$|IM\rangle = \sum_{K=-I}^I A_K |IMK\rangle. \quad (\text{B8})$$

However, there are symmetry conditions that cause the general Hamiltonian to have restrictions giving two groups of general solutions: those that have K quantum numbers all even and those that have them all odd. Additionally there are invariances as to the specific labelling of the body fixed axes. We consider the excited states for use in MCAS evaluations as being members of the collective model sets with lowest energies. This usually restricts consideration to the A-representation [39, 40] (for positive-parity states), whence $A_{-K} = (-)^I A_K$. If negative-parity states are required, then members of the B₁-representation, for which $A_{-K} = (-)^{I+1} A_K$, need be considered. For most even-mass nuclei, the ground state spin-parity is 0^+ and we restrict consideration to nuclear systems having axial symmetry.

The nuclear states considered then are eigenfunctions of the quantised rotor Hamiltonian

$$H = \frac{\hbar^2}{2} \left[\frac{1}{\mathcal{I}_0} L_1^2 + \frac{1}{\mathcal{I}_0} L_2^2 + \frac{1}{\mathcal{I}_3} L_3^2 \right] = \frac{\hbar^2}{2} \left[\frac{1}{\mathcal{I}_0} \mathbf{L}^2 + \left(\frac{1}{\mathcal{I}_3} - \frac{1}{\mathcal{I}_0} \right) L_3^2 \right], \quad (\text{B9})$$

which has eigenenergies given by

$$H|LMK\rangle = \frac{\hbar^2}{2} \left[\frac{1}{\mathcal{I}_0} L(L+1) + \left(\frac{1}{\mathcal{I}_3} - \frac{1}{\mathcal{I}_0} \right) K^2 \right] |LMK\rangle. \quad (\text{B10})$$

As we limit consideration to axial symmetric cases, we must impose invariance under rotation of 180° about any axis perpendicular to the symmetry axis. With $|IMK\rangle = D_{MK}^I(\xi)$ and incorporating the eigenstates of the intrinsic Hamiltonian [39, 40],

$$H_{intrinsic} \phi_K(\omega) = \epsilon_0(K) \phi_K(\omega), \quad (\text{B11})$$

the normalised eigenstates of interest are

$$\Psi_{I,MK}(\xi, \omega) = \sqrt{\frac{(2I+1)}{16\pi^2(1+\delta_{K0})}} \left[D_{MK}^I(\xi) \phi_K(\omega) + (-)^{(I+K)} D_{M,-K}^I(\xi) \phi_{\bar{K}}(\omega) \right]. \quad (\text{B12})$$

Here \bar{K} is defined from the symmetry requirement

$$\phi_{\bar{K}}(\omega) = \mathcal{R}_2(-\pi) \phi_K(\omega) = e^{i\pi J_2} \phi_K(\omega) = \pm \phi_K(\omega) \quad \text{as } I \text{ is even/odd.} \quad (\text{B13})$$

Let $r_I (= \pm 1)$ be the eigenvalues of Eq. (B13).

In the specification of the coupled-channel potentials for MCAS, reduced matrix elements of Y_{LM}^* , with angles relating to the body-fixed axes, are required. Furthermore we assume that the intrinsic state does not change for low-excitation spectra. Matrix elements with

states given in Eq. (B12) then are

$$\begin{aligned}
\langle \Psi_{NK}^I | Y_{LM}^* | \Psi_{N'K'}^{I'} \rangle = & \frac{1}{16\pi^2} \sqrt{\frac{(2I+1)(2I'+1)}{(1+\delta_{K0})(1+\delta_{K'0})}} \left\{ \langle D_{NK}^I | Y_{LM}^* | D_{N'K'}^{I'} \rangle \delta_{KK'} \right. \\
& + (-)^{(I+I'+K+K')} \langle D_{N,-K}^I | Y_{LM}^* | D_{N',-K'}^{I'} \rangle r_I r_{I'} \delta_{\bar{K}\bar{K}'} \\
& + (-)^{(I+K)} \langle D_{N,-K}^I | Y_{LM}^* | D_{N'K'}^{I'} \rangle r_I \delta_{\bar{K}\bar{K}'} \\
& \left. + (-)^{(I'+K')} \langle D_{NK}^I | Y_{LM}^* | D_{N',-K'}^{I'} \rangle r_{I'} \delta_{K\bar{K}} \right\}. \quad (B14)
\end{aligned}$$

As

$$\begin{aligned}
Y_{LM}^*(\beta, \alpha) &= \sqrt{\frac{(2L+1)}{4\pi}} D_{M0}^L(\alpha, \beta, \gamma) \\
\langle D_{NK}^I | D_{M0}^L | D_{N'K'}^{I'} \rangle &= \frac{8\pi^2}{(2I+1)} \langle I'LN'M | IN \rangle \langle I'LK'0 | IK \rangle \delta_{K'K}, \quad (B15)
\end{aligned}$$

the matrix elements reduce to

$$\begin{aligned}
\langle \Psi_{NK}^I | Y_{LM}^* | \Psi_{N'K'}^{I'} \rangle &= \sqrt{\frac{(2I'+1)(2L+1)}{4\pi(2I+1)}} \langle I'LN'M | IN \rangle \\
&\times \frac{1}{2} \frac{1}{(1+\delta_{K0})} \left\{ \langle I'LK0 | IK \rangle + (-)^{(I+I')} \langle I'L-K0 | I-K \rangle r_I r_{I'} \right. \\
&\left. + (-)^{(I+K)} \langle I'L-K0 | IK \rangle r_{I'} + (-)^{(I'+K)} \langle I'LK0 | I-K \rangle r_I \right\}. \quad (B16)
\end{aligned}$$

The latter two terms contribute only for $K=0$ and so offset the factor $(1+\delta_{K0})^{-1}$. The reduced matrix elements are then identified by

$$\begin{aligned}
\langle \Psi_K^I || Y_L || \Psi_{N'}^{I'} \rangle &= \frac{1}{2} \sqrt{\frac{(2I'+1)(2L+1)}{4\pi}} \frac{1}{(1+\delta_{K0})} \\
&\times \left\{ \langle I'LK0 | IK \rangle \left[1 + (-)^{(I+I')} r_I r_{I'} \right] + \delta_{K0} \langle I'L00 | I0 \rangle \left[(-)^I r_I + (-)^{I'} r_{I'} \right] \right\} \\
&= \sqrt{(2I'+1)} \frac{1}{(1+\delta_{K0})} \left\{ \langle I'LK0 | IK \rangle + \delta_{K0} \langle I'L00 | I0 \rangle \right\}, \quad (B17)
\end{aligned}$$

as $(-)^I r_I = +1$ in all cases as evident from Eq. (B13). Thus,

$$\langle \Psi_K^I || Y_L || \Psi_{N'}^{I'} \rangle = \sqrt{\frac{(2I'+1)(2L+1)}{4\pi}} \langle I'LK0 | IK \rangle. \quad (B18)$$

For the $N=Z$ nuclei considered, the intrinsic energy is taken to be zero, and the strongly coupled states are taken to be the $K=0$ ground state. The structure factors are then simply the reduced matrix elements of three spherical harmonics.

Appendix C: Using a vibration model of the nucleus

The surface of a liquid drop of incompressible fluid that can be slightly deformed is represented as

$$R(\theta\phi) = R_0 \left[\alpha_{00}^* + \sum_{\lambda\mu} \alpha_{\lambda\mu}^* Y_{\lambda\mu}(\theta\phi) \right], \quad (\text{C1})$$

which, though similar to Eq. (B2), has important differences. As the radius must be a real quantity, the coefficients must satisfy the spherical harmonic identity, $\alpha_{\lambda\mu}^* \equiv (-)^\mu \alpha_{\lambda-\mu}$. The center of mass is defined by

$$M\mathbf{R} = \sum_i m_i \mathbf{r}_i = \int \rho_m \mathbf{R} d\mathbf{r},$$

where ρ_m is the mass density assumed to be uniform. Considering the z -component of the center of mass coordinate, $Z = r \cos(\theta)$, which must be zero in the center of mass frame, we find

$$\begin{aligned} MZ &= \sqrt{\frac{4\pi}{3}} \rho_m \int Y_{10}^*(\Omega) r^2 dr d\Omega \\ &= \sqrt{\frac{4\pi}{3}} \rho_m \frac{1}{4} R_0^4 \int Y_{10}^*(\Omega) \left[\alpha_{00}^* + \sum_{\lambda\mu} \alpha_{\lambda\mu}^* Y_{\lambda\mu}(\theta\phi) \right]^3 d\Omega \\ &\simeq \sqrt{\frac{4\pi}{3}} \rho_m R_0^4 [\alpha_{00}^*]^3 \alpha_{10}^* \quad (\text{to first order}). \end{aligned} \quad (\text{C2})$$

As α_{00} is of order unity, for Z to be zero, α_{10}^* must vanish. Hence, with a single fluid model, there can be no dipole ($\lambda = 1$) component in the expansion of the surface. Finally, as it is assumed that the drop is of incompressible matter, the volume should remain constant. This gives the constraint,

$$\begin{aligned} 1 &= \frac{3}{4\pi R_0^3} \int r^2 dr d\Omega = \frac{1}{4\pi} \int \left[\alpha_{00}^* + \sum_{\lambda>1,\mu} \alpha_{\lambda\mu}^* Y_{\lambda\mu}(\theta\phi) \right]^3 d\Omega \\ &= [\alpha_{00}^*]^3 + \frac{3}{4\pi} \alpha_{00}^* \sum_{\lambda>1,\mu} |\alpha_{\lambda\mu}|^2 + \dots \end{aligned} \quad (\text{C3})$$

Thus $\alpha_{00} = 1$ with correction only at second and higher orders so that we take,

$$R(\theta\phi) = R_0 \left[1 + \sum_{\lambda>1,\mu} \alpha_{\lambda\mu}^* Y_{\lambda\mu}(\theta\phi) \right]. \quad (\text{C4})$$

With this specification of the nuclear surface, expansion to second order in deformation of any function gives,

$$\begin{aligned} f(r) &= f_0(r) - R_0 \frac{df_0(r)}{dr} \sum_{\lambda\mu} \alpha_{\lambda\mu}^* Y_{\lambda\mu}(\theta\phi) \\ &\quad + \frac{1}{2} R_0^2 \frac{d^2 f_0(r)}{dr^2} \sum_{l_1 m_1 l_2 m_2} \alpha_{l_1 m_1}^* \alpha_{l_2 m_2}^* Y_{l_1 m_1}(\theta\phi) Y_{l_2 m_2}(\theta\phi). \end{aligned} \quad (\text{C5})$$

Therein, and in all that follows, it is presumed that summation of the expansion labels of the generalised coordinates, and subsequently of the angular momentum quantum numbers of the phonon creation/annihilation operators derived from them, exclude dipole terms, i.e. $\lambda > 1$.

The product of two generalised coordinates that satisfy the spherical harmonic condition, then can be written as,

$$\begin{aligned}\alpha_{l_1 m_1}^* \alpha_{l_2 m_2}^* &= \sum_{\nu_1 \nu_2} \delta_{m_1 \nu_1} \delta_{m_2 \nu_2} \alpha_{l_1 \nu_1}^* \alpha_{l_2 \nu_2}^* \\ &= \sum_{\lambda \mu} \langle l_1 l_2 m_1 m_2 | \lambda \mu \rangle \left[\sum_{\nu_1 \nu_2} \langle l_1 l_2 \nu_1 \nu_2 | \lambda \mu \rangle \alpha_{l_1 \nu_1}^* \alpha_{l_2 \nu_2}^* \right] \\ &= \sum_{\lambda \mu} \langle l_1 l_2 m_1 m_2 | \lambda \mu \rangle [\alpha_{l_1}^* \otimes \alpha_{l_2}^*]_{\lambda \mu} .\end{aligned}\tag{C6}$$

This form is convenient since $[\alpha_{l_1}^* \otimes \alpha_{l_2}^*]_{\lambda \mu}$ is a component of an irreducible tensor so that the second order term in Eq. (C5) can be written as

$$\begin{aligned}T_2 &= \frac{1}{2} R_0^2 \frac{d^2 f_0(r)}{dr^2} \sum_{l_1 m_1 l_2 m_2 \lambda \mu K} \langle l_1 l_2 m_1 m_2 | \lambda \mu \rangle [\alpha_{l_1}^* \otimes \alpha_{l_2}^*]_{\lambda \mu} \\ &\quad \times \sqrt{\frac{(2l_1 + 1)(2l_2 + 1)}{4\pi(2K + 1)}} \langle l_1 l_2 00 | K 0 \rangle \langle l_1 l_2 m_1 m_2 | K M_K \rangle Y_{KM_K}(\Omega) ,\end{aligned}\tag{C7}$$

and which on using the orthogonality of Clebsch-Gordan coefficients reduces to

$$T_2 = \frac{1}{2} R_0^2 \frac{d^2 f_0(r)}{dr^2} \sum_{\lambda} \sqrt{\frac{(2l_1 + 1)(2l_2 + 1)}{4\pi(2\lambda + 1)}} \langle l_1 l_2 00 | \lambda 0 \rangle [\alpha_{l_1}^* \otimes \alpha_{l_2}^*]_{\lambda} \cdot \mathbf{Y}_{\lambda}(\Omega) ,\tag{C8}$$

since the generalised coefficients must satisfy the spherical harmonic condition.

Thus, matrix elements of the type,

$$\begin{aligned}[f(r)]_{cc'} &= [f_0(r)]_{cc'} - R_0 \frac{df_0(r)}{dr} \left[\sum_{\lambda} [\alpha_{\lambda}^* \cdot \mathbf{Y}_{\lambda}(\Omega)] \right]_{cc'} \\ &\quad + \frac{1}{2} R_0^2 \frac{d^2 f_0(r)}{dr^2} \left[\sum_{l_1, l_2, \lambda} \sqrt{\frac{(2l_1 + 1)(2l_2 + 1)}{4\pi(2\lambda + 1)}} \langle l_1 l_2 00 | \lambda 0 \rangle [\alpha_{l_1}^* \otimes \alpha_{l_2}^*]_{\lambda} \cdot \mathbf{Y}_{\lambda}(\Omega) \right]_{cc'}\end{aligned}\tag{C9}$$

are found. The $\alpha_{\ell_i, m_{\ell_i}}$ are generalised (target) coordinates that are quantised to be a combination of phonon creation and annihilation operators, i.e.

$$\alpha_{\lambda \mu} \Rightarrow \frac{1}{\sqrt{(2\lambda + 1)}} \beta_{\lambda} \left[b_{\lambda \mu} + (-)^{\mu} b_{\lambda - \mu}^{\dagger} \right] ,\tag{C10}$$

where β_{λ} is the distortion parameter in this model. Note that this specification differs in form and scale from the development with rotation models. A quantal phonon of vibration is created/annihilated by the action of b_{LM}^{\dagger}/b_{LM} on any initial state. Thus, unlike the simpler

rotation model, in this case we need to specify expectation values of one and two phonon operators connecting states described appropriately. They are considered later.

Later it is convenient to use the generalised forms,

$$\begin{aligned} Q_{\lambda\mu}^{(1)} &= \alpha_{\lambda\mu} \\ Q_{\lambda\mu}^{(2)} &= \sum_{l_1 l_2} \sqrt{\frac{(2l_1+1)(2l_2+1)}{4\pi(2\lambda+1)}} \langle l_1 l_2 00 | \lambda 0 \rangle [\alpha_{l_1}^* \otimes \alpha_{l_2}^*]_{\lambda\mu}. \end{aligned} \quad (C11)$$

Using the basic interaction potential form given in Eqs. (6-9), the MCAS interaction matrix for the vibration model is

$$\begin{aligned} \{V\}_{cc'} &= \left[\left(V_0 + V_{\ell\ell} \ell(\ell+1) \right) f_0(r) + \frac{1}{2} V_{\ell I} \left(J(J+1) - \ell(\ell+1) - I(I+1) \right) g_0(r) \right] \delta_{cc'} \\ &\quad - R_0 \left[\frac{df_0(r)}{dr} \left(V_0 + \frac{1}{2} V_{\ell\ell} [\ell'(\ell'+1) + \ell(\ell+1)] \right) \right. \\ &\quad \left. + \frac{1}{4} V_{\ell I} \frac{dg_0(r)}{dr} \left(2J(J+1) - \ell'(\ell'+1) - \ell(\ell+1) - I'(I'+1) - I(I+1) \right) \right] \\ &\quad \times \sum_L [\alpha_L^* \cdot \mathbf{Y}_L]_{cc'} \\ &\quad + \frac{1}{2} R_0^2 \left[\frac{d^2 f_0(r)}{dr^2} \left(V_0 + \frac{1}{2} V_{\ell\ell} [\ell'(\ell'+1) + \ell(\ell+1)] \right) \right. \\ &\quad \left. + \frac{1}{4} V_{\ell I} \frac{d^2 g_0(r)}{dr^2} \left(2J(J+1) - \ell'(\ell'+1) - \ell(\ell+1) - I'(I'+1) - I(I+1) \right) \right] \\ &\quad \times \sum_{\lambda} \left[\left\{ \sum_{l_1 l_2} Q_{\lambda}^{(2)}(l_1, l_2) \right\} \cdot \mathbf{Y}_{\lambda} \right]_{cc'}, \end{aligned} \quad (C12)$$

where

$$Q_{\lambda}^{(2)}(l_1 l_2) = \sqrt{\frac{(2l_1+1)(2l_2+1)}{4\pi(2\lambda+1)}} \langle l_1 l_2 00 | \lambda 0 \rangle [\alpha_{l_1}^* \otimes \alpha_{l_2}^*]_{\lambda}. \quad (C13)$$

The first and second order terms require development as matrix elements of nuclear phonon operators. With scalar operators, $[\mathcal{X}_{\mathbf{L}} \cdot \mathbf{Y}_L(\Omega)]_{0,0}$, using the identity, (Eq. (5.13) in [41]), suitably adjusted to Edmond's form for the Wigner-Eckart theorem,

$$\begin{aligned} \langle c | [\mathcal{X}_{\mathbf{L}} \cdot \mathbf{Y}_L(\Omega)]_{0,0} | c' \rangle &= \frac{1}{\sqrt{(2J+1)}} \langle (\ell I) J \| [\mathcal{X}_{\mathbf{L}} \cdot \mathbf{Y}_L(\Omega)]_0 \| (\ell' I') J \rangle \\ &= (-)^{(\ell'+I+J)} \left\{ \begin{matrix} \ell & \ell' & L \\ I' & I & J \end{matrix} \right\} \langle \ell \| Y_L \| \ell' \rangle \langle I \| \mathcal{X}_L \| I' \rangle \\ &= (-)^{(\ell'+I+J)} \left\{ \begin{matrix} \ell & \ell' & L \\ I' & I & J \end{matrix} \right\} \sqrt{\frac{(2L+1)(2\ell'+1)}{4\pi}} \langle \ell' L 00 | \ell 0 \rangle \langle I \| \mathcal{X}_L \| I' \rangle, \end{aligned} \quad (C14)$$

since

$$\langle \ell \| Y_L \| \ell' \rangle = \sqrt{\frac{(2L+1)(2\ell'+1)}{4\pi}} \langle \ell' L 00 | \ell 0 \rangle. \quad (C15)$$

With the above, Eq. (C12) expands to

$$\begin{aligned}
\{V\}_{cc'} = & \left[\left(V_0 + V_{\ell\ell}\ell(\ell+1) \right) f_0(r) + \frac{1}{2}V_{\ell I} \left(J(J+1) - \ell(\ell+1) - I(I+1) \right) g_0(r) \right] \delta_{cc'} \\
& - R_0 \left[\frac{df_0(r)}{dr} \left(V_0 + \frac{1}{2}V_{\ell\ell} [\ell'(\ell'+1) + \ell(\ell+1)] \right) \right. \\
& \quad \left. + \frac{1}{4}V_{\ell I} \frac{dg_0(r)}{dr} [2J(J+1) - \ell'(\ell'+1) - \ell(\ell+1) - I'(I'+1) - I(I+1)] \right] \\
& \quad \times (-)^{(\ell'+I+J)} \sum_L \left\{ \begin{matrix} \ell & \ell' & L \\ I' & I & J \end{matrix} \right\} \sqrt{\frac{(2L+1)(2\ell'+1)}{4\pi}} \\
& \quad \times \langle \ell' L 0 0 | \ell 0 \rangle \langle I \| \alpha_L^* \| I' \rangle \\
& + \frac{1}{8\pi} R_0^2 \left[\frac{d^2 f_0(r)}{dr^2} \left(V_0 + \frac{1}{2}V_{\ell\ell} [\ell'(\ell'+1) + \ell(\ell+1)] \right) \right. \\
& \quad \left. + \frac{1}{4}V_{\ell I} \frac{d^2 g_0(r)}{dr^2} \left(2J(J+1) - \ell'(\ell'+1) - \ell(\ell+1) - I'(I'+1) - I(I+1) \right) \right] \\
& \quad \times (-1)^{(\ell'+I+J)} \sum_\lambda \sqrt{4\pi(2\ell'+1)(2\lambda+1)} \langle \ell' \lambda 0 0 | \ell 0 \rangle \\
& \quad \times \left\{ \begin{matrix} \ell & \ell' & \lambda \\ I' & I & J \end{matrix} \right\} \langle I \| Q_\lambda^{(2)} \| I' \rangle. \quad (C16)
\end{aligned}$$

-
- [1] I. J. Thompson and F. M. Nunes, *Nuclear Reactions for Astrophysics* (Cambridge University Press, New York, 2009).
 - [2] W. von Oertzen, M. Freer, and Y. Kanada-En'yo, Phys. Rep. **432**, 43 (2006).
 - [3] M. Freer, Rep. Prog. Phys. **70**, 2149 (2007).
 - [4] T. Myo, Y. Kikuchi, H. Masui, and K. Kato, Prog. Part. Nucl. Phys. **79**, 1 (2014).
 - [5] H. Yépez-Martínez, M. J. Ermamatov, P. R. Fraser, and P. O. Hess, Phys. Rev. C **86**, 034309 (2012).
 - [6] H. Yépez-Martínez, P. R. Fraser, P. O. Hess, and G. Lévai, Phys. Rev. C **85**, 014316 (2012).
 - [7] P. R. Fraser, H. Yépez-Martínez, P. O. Hess, and G. Lévai, Phys. Rev. C **85**, 014317 (2012).
 - [8] Y. Kanada-En'yo, Phys. Rev. C **89**, 024302 (2014).
 - [9] K. Amos, L. Canton, G. Pisent, J. P. Svenne, and D. van der Knijff, Nucl. Phys. **A728**, 65 (2003), and references cited therein.
 - [10] D. R. Tilley, J. H. Kelley, J. L. Godwin, D. J. Millener, J. E. Purcell, C. G. Sheu, and H. R. Weller, Nucl. Phys. **A745**, 155 (2004).
 - [11] F. Ajzenberg-Selove, Nucl. Phys. **A 506**, 1 (1990).
 - [12] D. R. Tilley, H. R. Weller, and C. M. Cheves, Nucl. Phys. **A 564**, 1 (1993).
 - [13] D. R. Tilley, C. M. Cheves, J. H. K. S. Raman, and H. R. Weller, Nucl. Phys. **A 636**, 247 (1998).
 - [14] P. Fraser, K. Amos, L. Canton, G. Pisent, S. Karataglidis, J. Svenne, and D. van der Knijff, Phys. Rev. Lett. **101**, 242501 (2008).
 - [15] L. Canton, P. R. Fraser, J. P. Svenne, K. Amos, S. Karataglidis, and D. van der Knijff, Phys. Rev. C **83**, 047603 (2011).

- [16] L. Canton, G. Pisent, K. Amos, S. Karataglidis, J. P. Svenne, and D. van der Knijff, Phys. Rev. C **74**, 064605 (2006).
- [17] G. Cattapan, L. Canton, and G. Pisent, Phys. Rev. C **43**, 1395 (1991), and references cited therein.
- [18] G. Pisent and J. P. Svenne, Phys. Rev. C **51**, 3211 (1995).
- [19] L. Canton, G. Pisent, J. P. Svenne, D. van der Knijff, K. Amos, and S. Karataglidis, Phys. Rev. Lett **94**, 122503 (2005).
- [20] V. Krasnopol'sky and V. Kukulin, Soviet J. Nucl. Phys. **20**, 883 (1974).
- [21] V. Kukulin and V. Pomerantsev, Ann. of Phys. **111**, 330 (1978).
- [22] S. Saito, Prog. Theor. Phys. **41**, 705 (1969).
- [23] W. Horiuchi and Y. Suzuki, J. Phys.: Conference series **436**, 012031 (2013).
- [24] E. W. Schmid, in *Proceedings of the workshop in few-body problems in nuclear physics* (Trieste, Italy, 1978), p. 389.
- [25] L. Canton, G. Pisent, J. P. Svenne, K. Amos, and S. Karataglidis, Phys. Rev. Lett. **96**, 072502 (2006).
- [26] K. Amos, L. Canton, S. Karataglidis, J. P. Svenne, D. van der Knijff, and P. R. Fraser, Nucl. Phys. **A879**, 132 (2012).
- [27] K. Amos, L. Canton, P. R. Fraser, S. Karataglidis, J. P. Svenne, and D. van der Knijff, Nucl. Phys. **A912**, 7 (2013).
- [28] R. B. Firestone et al., *Table of Isotopes* (John Wiley & Sons, New York, 1996), eighth ed.
- [29] D. R. Tilley et al., Nucl. Phys. **A 708** (2002).
- [30] G. Audi, A. H. Wapstra, and C. Thibault, Nucl. Phys. A **729**, 337 (2003).
- [31] Y. Suzuki, Prog. Theor. Phys. **55**, 1751 (1976).
- [32] Y. Suzuki, Prog. Theor. Phys. **56**, 111 (1976).
- [33] K. Ikeda, H. Horiuchi, and S. Saito, Prog. Theor. Phys. Suppl. **86**, 1 (1980).
- [34] M. Libert-Heinemann, D. Baye, and P.-H. Heenen, Nucl. Phys. **A 339** (1980).
- [35] I. Mukha et al., Phys. Rev. C **79**, 061301 (2009).
- [36] I. Mukha et al., Phys. Rev. C **82**, 054315 (2010).
- [37] J. Demarche and G. Terwagne, J. App. Phys. **100**, 124909 (2006).
- [38] R. A. Jarjis, J. Nucl. Inst. Meth. B **12**, 331 (1985).
- [39] J. P. Davidson, *Collective models of the nucleus* (Academic Press, New York, 1968).
- [40] D. J. Rowe, *Nuclear collective motion; models and theory* (Methuen, London, 1970).
- [41] D. M. Brink and G. R. Satchler, *Angular Momentum* (Clarendon Press, Oxford, 1968).